Modeling Bi-induced changes in the electronic structure of GaAs$_{1-x}$Bi$_x$ alloys

Ville Virkkala, Ville Havu, Filip Tuomisto, and Martti J. Puska

COMP, Department of Applied Physics, Aalto University, P.O. Box 11100, FI-00076 Aalto, Finland

We suggested recently [V. Virkkala *et al.*, Phys. Rev. B **88**, 035204 (2013)] that the band-gap narrowing in dilute GaAs$_{1-x}$N$_x$ alloys can be explained to result from the broadening of the localized N states due to the N-N interaction along the zigzag chains in the $\langle 110 \rangle$ directions. In that study our tight-binding modeling based on first-principles density-functional calculations took into account the random distribution of N atoms in a natural way. In this work we extend our modeling to GaAs$_{1-x}$Bi$_x$ alloys. Our results indicate that Bi states mix with host material states. However, the states near the valence-band edge agglomerate along the zigzag chains originating from individual Bi atoms. This leads to Bi-Bi interactions in a random alloy broadening these states in energy and causing the band-gap narrowing.

PACS number(s): 71.20.Nr, 61.72.uj, 71.15.Mb, 71.55.Eq

I. INTRODUCTION

It is well known that in GaAs$_{1-x}$N$_x$ alloys already a dilute amount of N atoms substituting the As atoms causes significant modifications on the electronic structure of the material.[1,2] These modifications are observed as the narrowing of the band gap of the host material at low-N concentrations[3] and as an anomalously heavy electron mass.[4] The tunability of the band gap at low-N concentrations enables many applications in optical telecommunications as well as in solar cell technology.[5] The band-gap narrowing is also observed in the case of GaAs$_{1-x}$Bi$_x$ alloys and currently the focus in research is shifted towards GaAs$_{1-x}$Bi$_x$. Bi alloying of GaAs is appealing because of the small size mismatch between As and Bi, which should make it easier to produce materials with good electronic properties in contrast to GaAs$_{1-x}$N$_x$ alloys, for which, e.g., the electron mobility significantly decreases.[6]

In GaAs$_{1-x}$Bi$_x$ alloys also a significant spin-orbit (SO) splitting is observed[7] and it is reported that the SO splitting energy might become larger than the band gap of the alloy, i.e., $\Delta_{SO} > E_g$.[8] This phenomenon, together with a relatively large band gap, could enable new possibilities for the near infrared lasers, due to the damping of the Auger recombination processes from the valence-band edge (VBE) into the SO split-off band.[8] Recently, the electromodulation spectroscopy measurements by Kudrawiec *et al.* have enlightened the behavior of the SO splitting in the GaAs$_{1-x}$Bi$_x$ alloys.[9] They determined the widths and intensities of the electric transitions E_0 and $E_0 + \Delta_{SO}$ from the top of the valence band and from the top of the split-off band, respectively, to the bottom of the conduction band. They found that by inserting Bi into alloy the E_0 transition broadens strongly and its relative intensity decreases in comparison to the $E_0 + \Delta_{SO}$ transition. The E_0 transition experienced also a much stronger redshift than the $E_0 + \Delta_{SO}$ transition. Kudrawiec *et al.* concluded that the heavy/light hole band at the top of the valence band broadens due to the alloy inhomogeneities and Bi atom complexes whereas the SO band and the bottom of the conduction band are less affected.[9]

The band-gap narrowing in dilute N-doped III-V semiconductor alloys is often explained using the band anticrossing (BAC) model.[10] According to the BAC model for GaAs$_{1-x}$N$_x$ alloys, the resonant N state above the bulk conduction-band edge (CBE) pushes the CBE downwards causing the band-gap narrowing. In GaAs$_{1-x}$Bi$_x$ alloys the Bi states are formed on the valence band and the VBE is instead pushed upwards causing the band-gap narrowing which is described using the valence-band anticrossing (VBAC) model.[11] This phenomenon can also be observed in other Bi alloyed III-V semiconductors such as GaP$_{1-x}$Bi$_x$.[12] In contrast to the BAC model, it was recently suggested that the band-gap narrowing results from the interactions and the ensuing broadening of the localized Bi p^* states or N s^* states in GaAs$_{1-x}$Bi$_x$ and GaAs$_{1-x}$N$_x$ alloys, respectively.[13] Similar explanations were also given in Ref. 14 in the case of GaP$_{1-x}$N$_x$ alloys. We studied this explanation recently in a quantitative manner in the case of GaAs$_{1-x}$N$_x$ and GaP$_{1-x}$N$_x$ alloys.[15] We found that the CBE charge density agglomerates along the zigzag chains on the $\langle 110 \rangle$ directions and our tight-binding (TB) model for N-N interactions led to a broadening of the N localized states in a quantitative accordance with experiments.[16]

The publishing rate of computational and experimental studies considering GaAs$_{1-x}$Bi$_x$ alloys has speeded up drastically during the recent years. One of the earliest *ab initio* studies considering Bi substitution in GaAs was performed by Janotti *et al.* in Ref. 17, where the density functional theory (DFT) within the local-density approximation (LDA) and the supercell (SC) approach were used. They concluded that the substitution of Bi together with N into GaAs would serve a potential 1-eV band-gap material lattice-matched to GaAs. In Ref. 18 Zhang *et al.* studied GaAs$_{1-x}$Bi$_x$ alloys in a non-self-consistent fashion using LDA and large SCs up to 4096 atoms. The band gaps they obtained as a function of the Bi concentration were in good agreement with experimental band gaps and they also reported a superlinear SO splitting with respect to the Bi concentration. Usman *et al.* performed a detailed computational study of GaAs$_{1-x}$Bi$_x$ and GaP$_{1-x}$Bi$_x$ alloys using a nearest-neighbor sp^3s^* TB Hamiltonian.[12] Their calculated band gaps and SO energies were in a good agreement with experiments. In Ref. 7 Fluegel *et al.* performed photoluminescence measurements of GaAs$_{1-x}$Bi$_x$ alloys. They reported a large relativistic correction to the electronic structure of the host material due to Bi atoms and suggested the possibility of tuning the SO splitting for semiconductor spintronic applications by altering the Bi concentration.

In this work we study $GaAs_{1-x}Bi_x$ alloys using the DFT approach including the SO coupling self-consistently. We show that in the case of $GaAs_{1-x}Bi_x$ alloys the Bi-induced perturbation in the host electronic structure is clearly smaller than that induced by N in $GaAs_{1-x}N_x$ alloys. N causes a well-distinguishable dispersionless band just above the bottom of the conduction band whereas the Bi-induced changes are quantitative modifications in the host valence band. However, the VBE density agglomerates strongly along zigzag chains originating from Bi atoms. The ensuing states, which we call *mixed Bi-bulk states*, are visible as a peak in the local density of states (LDOS) at the Bi atom. The agglomeration of the VBE charge density along the zigzag chains leads to Bi-Bi interactions (which are clearly seen in the splitting of the LDOS peak when two Bi atoms are located in neighboring anion sites). The oriented Bi-Bi interactions have a long range and in a random alloy they lead to the broadening of the mixed Bi-bulk states in the top of the valence band and to the band-gap narrowing.

In order to study the effects of a finite Bi concentration quantitatively, we extend our earlier TB model[15] for the random dilute III-V-N alloys to the random $GaAs_{1-x}Bi_x$ alloys. The parameters of the model are based on our DFT results for periodic supercells. We obtain a band-gap narrowing which is in agreement with experimental findings giving credence to our idea of directional, long-range interactions between Bi atoms. Moreover, our calculations suggest that the observed superlinear behavior of the SO splitting energy with respect to Bi concentration,[18] i.e., the observed SO splitting energy increases faster than the linear interpolation between the SO splitting energies of the end-point constituents of GaAs and GaBi, is due to the raising of the valence-band maximum (VBM). This follows from the broadening of the mixed Bi-bulk states near the VBE.

II. METHODS

All our DFT calculations are performed using the Vienna *ab initio* simulation package (VASP)[19] within the projector augmented wave (PAW) method[20]. The valence electron configurations used in the calculations, for Ga, As, and Bi are $4s^2 4p^1$, $4s^2 4p^3$, and $6s^2 6p^3$, respectively. The LDA is employed and the SO coupling is included in all calculations. The LDA approximation enables the use of large supercells and it describes qualitatively but also quantitatively correctly the Bi-induced changes in the valence-band states compared to our test calculations[21] performed with the HSE06 hybrid-functional which produces the experimental bulk band gap of 1.52 eV of GaAs at 0 K.[22] A cutoff energy of 400 eV is used for the plane-wave basis set providing the convergence of the total energy. The stopping criterion for ionic relaxation is that the forces acting on each atom are smaller than 0.02 eV/Å. The ionic relaxation is performed without the SO coupling. The studied systems are simple cubic $GaAs_{1-x}N_x$ SCs of 512, 216, and 64 atoms with a single Bi atom and a configuration containing two Bi atoms in the neighboring anion sites of the 216-atom supercell. A $2 \times 2 \times 2$ Monkhorst-Pack set is used for the **k**-point sampling in structural optimization and total-energy optimization in band-structure calculations. The densities of states (DOSs), in the case of a single Bi atom

in the supercell, are generated using Monkhorst-Pack sets of $3 \times 3 \times 3$, $5 \times 5 \times 5$, and $7 \times 7 \times 7$ **k**-points, corresponding to SCs of 512, 216, and 64 atoms, respectively, except for the SC containing two Bi atoms where a $3 \times 3 \times 3$ **k**-point set is used. The Brillouin-zone integration for DOS calculations is performed using the linear tetrahedron method. The lattice constants are optimized for different sizes of SCs containing Bi atoms, being just slightly larger than the calculated lattice constant of bulk GaAs (5.63 Å).

In order to simulate more realistic structures of randomly distributed Bi atoms, we extend our earlier TB model[15] for N atoms in III-V compound semiconductors to $GaAs_{1-x}Bi_x$ alloys. In the model the broadening of the mixed Bi-bulk states near the VBE arises from the interaction between Bi atoms. For two Bi atoms at positions $\hat{\mathbf{r}}_i$ and $\hat{\mathbf{r}}_j$, the interaction decays slowly as $k/r_{i,j}^{\alpha}$ if the Bi atoms are connected by a zigzag chain, and vanishes otherwise. In the SC and Γ-point approximations the matrix elements become[15]

$$h_{i,j} = \sum_{\phi} \sum_{n=0}^{\infty} \frac{k}{(r_{i,j_\phi} + \sqrt{2}nL)^{\alpha}}. \tag{1}$$

Above, ϕ runs over all the octants of space where the N atoms i and j are connected through a zigzag chain and L is the side length of the cubic SC. The diagonal terms become

$$h_{i,i} = E_{Bi} + 12 \sum_{n=1}^{\infty} \frac{k}{(\sqrt{2}nL)^{\alpha}}, \tag{2}$$

where E_{Bi} describes the energy of the mixed Bi-bulk states (see below). To determine the parameters k and α we use SCs comprising of up to several thousands of Bi atoms in our TB calculations. The Bi atoms in the SCs obey the same underlying periodicity as the structures in our SC-DFT calculations. We need to employ a large number of Bi atoms in the SCs to obtain a large enough number of eigenvalues in the Γ-point approximation for a converged eigenvalue distribution. We then solve these systems using our TB model and compare the results to our SC-DFT results in the case of four structures of a single Bi atom in the SCs of 64, 216, 512 atoms and of two Bi atoms at the neighboring anion sites in the 216-atom SC. We fit the eigenvalue distributions produced by our TB model to the Bi related features in our SC-DFT LDOSs at the Bi atom. In the case of a single Bi atom the fitted feature is the tail length, i.e., the distance between the peak maximum related to the mixed Bi-bulk states and the VBM. In the case of two Bi atoms at the neighboring anion sites the fitted features are the distance between the two peaks (due to the splitting of the single peak) and the distance between their center of mass and the VBM. The LDOSs at the Bi atom are shown and the Bi related features are explained below.

III. RESULTS AND DISCUSSION

A. DFT results for $GaAs_{1-x}Bi_x$ alloys in the SC approximation

Figures 1(a)–1(c) show the band structures in the case of bulk $Ga_{108}As_{108}$, $Ga_{108}As_{107}Bi$, and $Ga_{32}As_{31}Bi$, respectively. At the top of the valence band we see the heavy/light hole bands separated at the Γ point by the splitting Δ_{SO} from the SO band. For bulk GaAs $\Delta_{SO} = 0.35$ eV which is in a good agreement with the experimental value.[23] Increasing the Bi
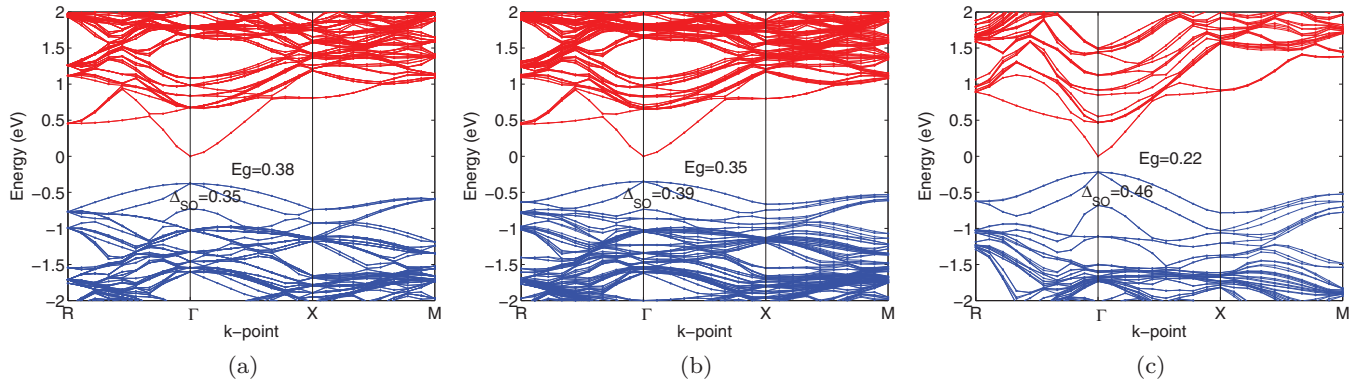
FIG. 1. (Color online) Band structures for bulk $Ga_{108}As_{108}$ (a), $Ga_{108}As_{107}Bi$ (b), and $Ga_{32}As_{31}Bi$ (c). The energy zero coincides with the CBM. The vertical lines are guides to the eye and indicate the positions of the high-symmetry points.

concentration increases Δ_{SO}. Figures 2(a)–2(c) show the p- and d-projected LDOSs at the Bi atom (the s-projected LDOS is in practice zero) in the alloy supercell and the total LDOSs at the As and Ga atoms in the corresponding bulk supercell in the case of $Ga_{256}As_{255}Bi$, $Ga_{108}As_{107}Bi$, and $Ga_{32}As_{31}Bi$, respectively. According to the LDOSs the Bi related states are located in the region from VBM down to around -1.5 eV below the (calculated) CBM. Especially the Bi atom enhances the LDOS near the VBM and a sharp peak appears (at the left ends of the solid bars drawn in the LDOS figures), that corresponds to the mixed Bi-bulk states. With increasing Bi concentration the peak starts to broaden and at the same time the VBE moves upwards around the Γ point. Figure 3(a) shows the p- and d-projected LDOSs at the Bi atom in the case of two Bi atoms at the neighboring anion sites in the $Ga_{108}As_{106}Bi_2$ SC. It is interesting to notice that in this case the peak related to the mixed Bi-bulk state is split into two peaks resembling the behavior in $GaAs_{1-x}N_x$ alloys.[15] As discussed above we fit our TB produced eigenvalue distributions to the distance of this peak from the VBM in the case of a single Bi atom in the SC and in the case of two Bi atoms at the neighboring anion sites in the SC to the positions of the two peaks and their distance from each others.

According to the band structures, Figs. 1(a)–1(c), the Bi atom does not induce new clearly impuritylike states, but creates mixed states with the bulk states reflecting the p-type bonding. This is in contrast to $GaAs_{1-x}N_x$ alloys where the substitution of an As atom by an N atom creates a flat impuritylike band of s character around the N atom and a sharp isolated peak is observed in the LDOS at the N atom.[15] The Bi-induced perturbations on the electronic band structure of the host material are minor and even the band structure of the high-Bi concentration $Ga_{32}As_{31}Bi$ resembles qualitatively that of bulk GaAs. On the other hand, in the case of two Bi atoms in neighboring anion sites the splitting of the LDOS peak at close to the top of the valence band signalizes clearly the interaction between states localized at Bi atoms.

In order to pinpoint the character of the states mediating the Bi-Bi interaction Fig. 4 shows the partial charge density of the VBE in $Ga_{256}As_{255}Bi$. The VBE charge density becomes strongly localized along the zigzag chains on the $\langle 110 \rangle$ direction after Bi substitution and at the same time the mixed Bi-bulk state near the VBE starts to broaden in energy [see Figs. 2(a)–2(c)]. This gives credence to the model proposed by Deng *et al.* in Ref. 13, where the interaction between Bi
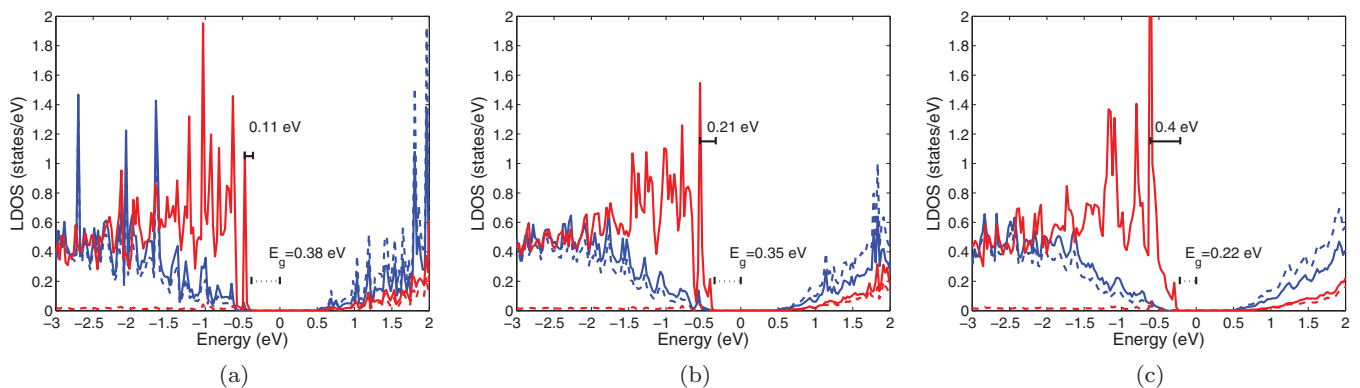

FIG. 2. (Color online) p-projected (solid red line) and d-projected (dashed red line) LDOSs at the Bi atom in the alloy supercell and the total LDOSs at the As (solid blue line) and Ga (dashed blue line) atoms in the corresponding bulk supercell in the case of $Ga_{256}As_{255}Bi$ (a), $Ga_{108}As_{107}Bi$ (b), and $Ga_{32}As_{31}Bi$ (c). To align the LDOSs of the alloy and bulk supercells the energy zero is set to CBM of the system. The solid segment indicates the distance between the peak related to the mixed Bi-bulk states and the VBM and the dashed segment indicates the calculated band gap of the alloy.
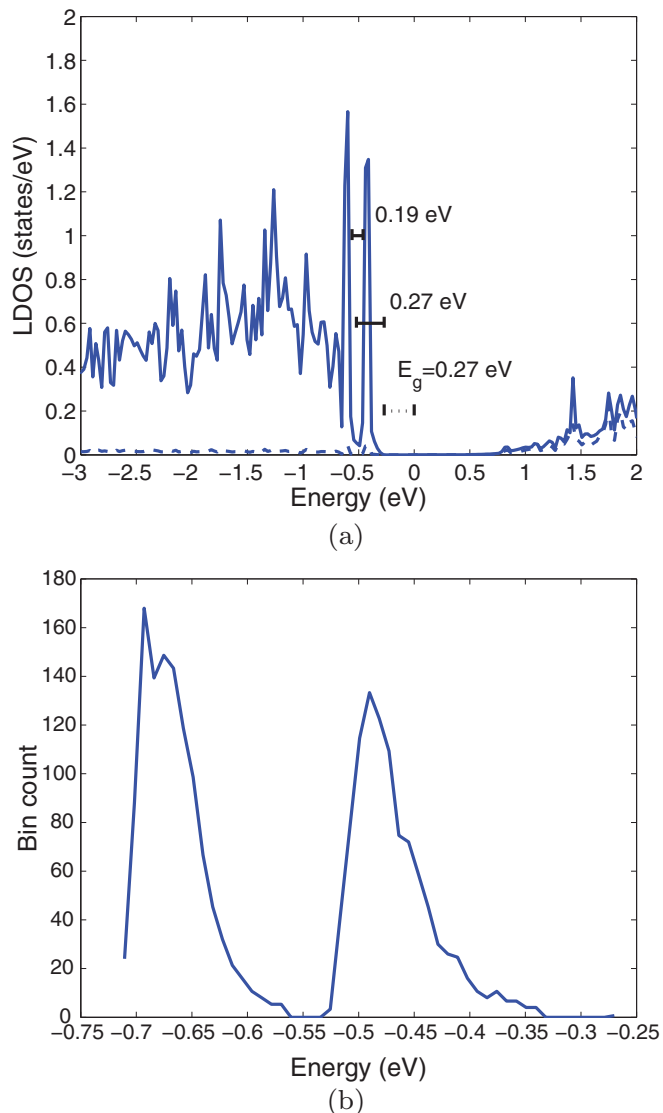
(a)

(b)

FIG. 3. (Color online) p-projected (solid line) and d-projected (dashed line) LDOSs at the Bi atom in the case of two Bi atoms at the neighboring anion sites in the Ga$_{108}$As$_{106}$Bi$_2$ SC (a) and a corresponding TB calculated eigenvalue distribution (smoothed using the moving average) (b). In (a) the solid segments indicate the distance between the two peaks and the distance between their center of mass and the VBM. The band gap is indicated by the dashed segment. The energy zero coincides with the CBM. In (b) the energy zero is set equal to the energy zero in (a).

atoms leads to the broadening of the localized Bi states and the narrowing of the band gap in GaAs$_{1-x}$Bi$_x$ alloys.

B. Tight-binding model for the directional Bi-Bi interaction and the band-gap narrowing in random GaAs$_{1-x}$Bi$_x$ alloys

To test our hypothesis about the directional Bi-Bi interaction as the origin of the band-gap narrowing in GaAs$_{1-x}$Bi$_x$ alloys against the experiments we calculate the band gap in random GaAs$_{1-x}$Bi$_x$ alloys using our developed TB model.[15] In Eq. (1) the parameter values $k = 0.85$ eV Å$^\alpha$, $\alpha = 1.55$ reproduce the Bi related features (see Sec. II) in the DFT-LDOSs at the Bi atom, shown in Figs. 2(a)–2(c) and 3(a). Figure 3(b)
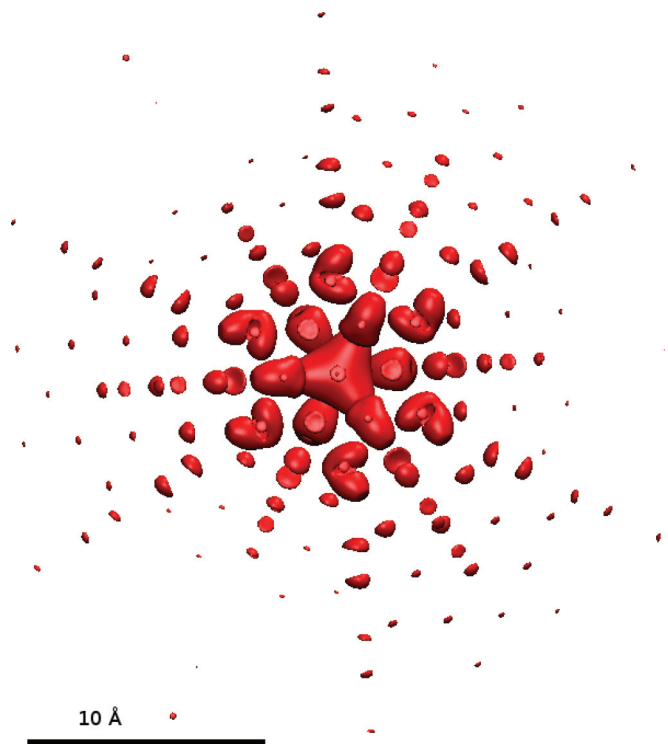

10 Å

FIG. 4. (Color online) VBE partial charge density in the case of Ga$_{256}$As$_{255}$Bi (density isovalue 0.000 24) viewed along the $\langle 111 \rangle$ direction. The Bi atom is located at the center of the figure.

shows, as an example, a fitted eigenvalue distribution produced by the implemented TB model in the case of two Bi atoms at the neighboring anion sites. The TB model reproduces the splitting of the SC-DFT calculated peak near the VBE shown in Fig. 3(a).

To simulate the broadening of the mixed Bi-bulk states near the VBE in real structures and the band-gap reduction as a function of Bi concentration, we randomly distribute from 48 up to 6636 Bi atoms into a SC of 55 296 anion sites. We approximate the lattice constant of the alloy at different Bi concentrations using Vegard's law $L_{\text{alloy}} = (1 - x)L_{\text{GaAs}} + xL_{\text{GaBi}}$, where $L_{\text{GaAs}} = 5.63$ Å and $L_{\text{GaBi}} = 6.27$ Å are the calculated lattice constants of the end-point constituents. By solving the eigenvalue distribution of the resulting Hamiltonian we obtain a broadened eigenvalue distribution around the original peak corresponding to mixed Bi-bulk states near the alloy VBE. Figure 5 shows as an example the distribution for a random sample with a concentration of 6.0%. In the plot the highest peak is due to isolated Bi atoms and the two side peaks are due to nearest-neighbor Bi pairs.

The band-gap reduction in random structures due to alloyed Bi atoms is calculated on the basis of our simulations as

$$\Delta E_g(x) = -\max\{s(x) - C, 0\} - bx. \qquad (3)$$

Above, x stands for the Bi-concentration percent, b is the CBM downwards shift per Bi-concentration percent originating from the Vegard's law, $s(x)$ is the splitting of the peak corresponding to the mixed Bi-bulk states near the alloy VBE in the random structures (i.e., the distance between the maximum eigenvalue and the highest peak in Fig. 5). For each concentration x, $s(x)$ is calculated by averaging over 50 random samples. C is the
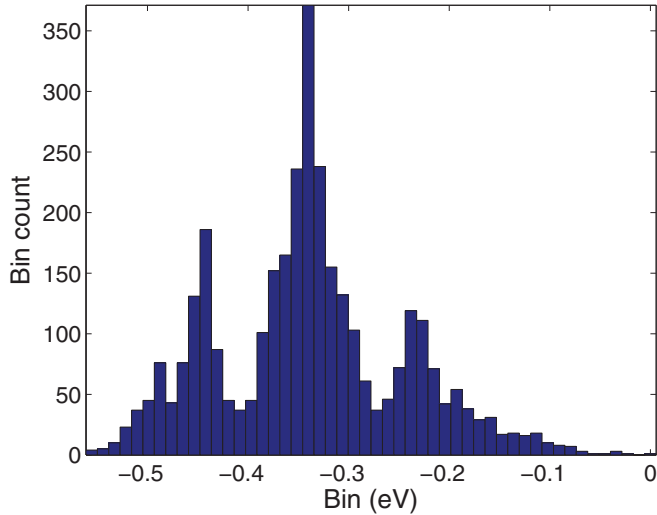
FIG. 5. (Color online) TB eigenvalue distribution corresponding to a random sample of 3318 Bi atoms on 55 296 anion sites (6.0% concentration) in the $GaAs_{1-x}Bi_x$ alloy. The energy zero is set equal to the maximum eigenvalue of the distribution.

distance of the peak corresponding to the mixed Bi-bulk states from the bulk VBM. For b we use a reported literature value of 28 meV/%.[12] The parameter C is obtained by requiring that Eq. (3) satisfies our SC-DFT results at different Bi concentrations shown in Figs. 1 and 2. The calculated value of C varies from 0.11 eV corresponding to the 512-atom supercell up to 0.33 eV corresponding to the 64-atom supercell. Here, for simplicity, an average value of 0.22 eV is used.

The calculated band gap, obtained using the experimental bulk GaAs band-gap value of Ref. 23 and the band-gap reduction from Eq. (3) is shown in Fig. 6 as a function of the Bi concentration together with the experimental data.[23]
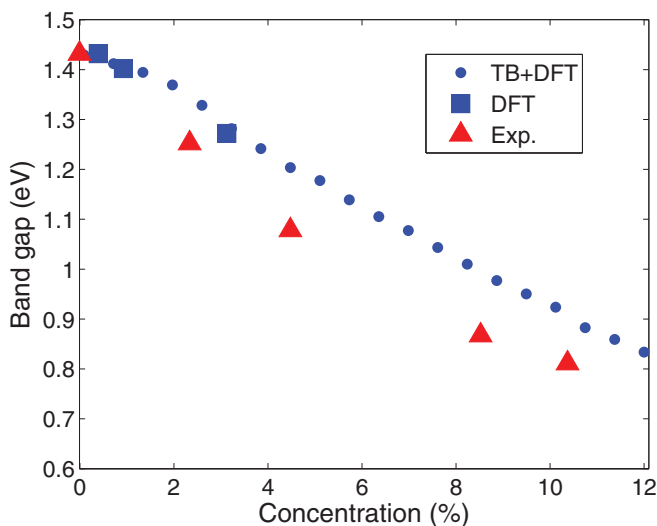

FIG. 6. (Color online) TB Calculated band gap (blue circles) based on Eq. (3), SC-DFT calculated band gap (blue squares) based on Figs. 1 and 2, and the experimental band gap (red triangles) in $GaAs_{1-x}Bi_x$ alloys as a function of Bi concentration. The experimental data are taken from Ref. 23 and it is measured at room temperature.

In addition the SC-DFT calculated band gap as determined on the basis of Figs. 1 and 2 is shown. According to Fig. 6 our model gives qualitatively and even quantitatively correct behavior of the band gap as a function of the Bi concentration.

C. Discussing the band-gap narrowing against earlier works

As mentioned above the strict position of the peak corresponding to mixed Bi-bulk states near the alloy VBE seems to decrease in energy with increasing Bi concentration and the strict location of the peak, with respect to bulk VBM, is a function of the Bi concentration x. Here, we used for simplicity a constant value for C based on the average value of our SC-DFT calculations. This creates some uncertainty to the predictive power of our model in the case of $GaAs_{1-x}Bi_x$ alloys. This is in contrast to $GaAs_{1-x}N_x$ alloys where the location of the N impurity state can be well defined. Our conclusions about the nature of the Bi states in the valence band resemble those by Zhang et al. in Ref. 18. Namely, they concluded that no new states are added into the valence band of GaAs and the Bi states could be interpreted as strongly perturbed host states. In addition, in Ref. 18 the location of the E_{Bi} state was found to vary with respect to the Bi concentration supporting our result on the behavior of the Bi-induced peak.

Remarkably, at small Bi concentrations, the SC-DFT calculations give a very similar band gap as our TB modeling for random systems. This is in a strong contrast to our corresponding calculations for $GaAs_{1-x}N_x$ and $GaP_{1-x}N_x$ alloys.[15] This is due to a compensation of the surplus of Bi-Bi interactions in periodic structures by the nearest-neighbor interactions in random structures due to large k and α values in the model. In addition, the lowering of the energy corresponding to the mixed Bi-bulk states peak with increasing Bi concentration compensates the increasing splitting of the mixed Bi-bulk states. This is not taken into account in our TB model. In $GaAs_{1-x}N_x$ and $GaP_{1-x}N_x$ alloys the SC-DFT calculations containing a single N atom lead to a significant overestimation of the broadening of the N induced states[15] and thus to a wrong concentration dependence of the band gap compared to experiments.

In Ref. 12 the authors use the fractional Γ character of wave functions to verify the validity of the VBAC model in $GaAs_{1-x}Bi_x$. They found that the fractional Γ character spreads over a range of energies below the VBM. The results in Ref. 12 are in agreement with our results and can be also well explained by our model. Near the zero concentration the significance of the zigzag chains nearly disappear, resulting in a very bulklike VBE, as is evident by comparing Figs. 1(a) and 1(b). With increasing Bi concentration the overlap between the zigzag charge chains becomes stronger leading to deteriorating bulk character in the alloy VBE and also to the interference with the lower-lying bulk states increases.

Our TB calculations for random Bi distributions produce a finite width of the VBM which is in accord with the concept of effective band structures with finite bandwidths introduced by Popescu and Zunger in Ref. 24. The finite width of the VBM is also in agreement with the observation by Kudrawiec et al. in Ref. 9 that the E_0 transition peak corresponding to band gap

broadens due to finite width of the VBM induced by adding Bi into GaAs.

D. Spin-orbit splitting in GaAs$_{1-x}$Bi$_x$ alloys

Our band-structure calculations [Figs. 1(a) and 1(b)] predict an increasing SO splitting energy as a function of the Bi concentration in agreement with previous computational and experimental results.[7,12,18] Especially our calculated SO splitting energies with respect to Bi concentration are in a good agreement with those of Zhang *et al.* in Ref. 18. However, our calculations do not show the occurrence of any extra states due to the SO splitting, as was suggested in Ref. 11, where two states were explicitly added and parametrized in analogy to the BAC model to reproduce the experimental SO splitting energy.

The interesting question related to the increasing SO splitting energy is that in which extent it is related to the actual SO coupling and in which extent to the VBM shifting upwards due to Bi-Bi interactions. Based on Figs. 1(a) and 1(c) the spin split-off bands remain in a rather constant energy level, from 0.72 eV up to 0.68 eV, below the calculated CBM in the bulk and Ga$_{32}$As$_{31}$Bi supercells, respectively. Thus, the increasing VBE upward shift due to Bi-Bi interactions would necessarily lead to increase in the observed SO splitting energy despite the SO coupling. This would explain the observed superlinear increase in the SO splitting energy with respect to Bi concentration.[18] The notion by Kudrawiec *et al.* in Ref. 9 that the position of the $E_0 + \Delta_{SO}$ transition peak is rather insensitive to the addition of 3% Bi into GaAs supports our view that the observed increase of the SO splitting is due to the shift of the VBM.

IV. CONCLUSIONS

In this work we performed DFT calculations for GaAs$_{1-x}$Bi$_x$ alloys including the SO coupling. Our calculations indicate that instead of forming a narrow impurity band the Bi states mix with bulk states in a wide energy region down to -1.5 eV below the (calculated) CBM. Our calculations also show that due to the Bi substitution the mixed Bi-bulk states near the VBM become agglomerated along the zigzag chains in the $\langle 110 \rangle$ directions, leading to a broadening of these states near the Γ point and to an upwards shift of the VBE causing the band-gap reduction. Our TB simulations for random alloy systems, describing the directional agglomeration of the mixed Bi-bulk states near the VBM, reproduce qualitatively and rather well quantitatively the experimentally observed band-gap reduction. Thus, we have successfully generalized our modeling ideas[15] from III-V-N alloys to the GaAs$_{1-x}$Bi$_x$ alloy.

Our DFT calculations also show an increasing SO splitting energy with increasing Bi concentration. Our results indicate that the large increase of the SO splitting energy with respect to Bi concentration is mainly caused by the VBE upward shift rather than being a relativistic effect.

[1] P. R. C. Kent and A. Zunger, Phys. Rev. B **64**, 115208 (2001).

[2] V. Virkkala, V. Havu, F. Tuomisto, and M. J. Puska, Phys. Rev. B **85**, 085134 (2012).

[3] L. Ivanova, H. Eisele, M. P. Vaughan, Ph. Ebert, A. Lenz, R. Timm, O. Schumann, L. Geelhaar, M. Dähne, S. Fahy, H. Riechert, and E. P. O'Reilly, Phys. Rev. B **82**, 161201 (2010).

[4] Y. Zhang, A. Mascarenhas, H. P. Xin, and C. W. Tu, Phys. Rev. B **61**, 7479 (2000).

[5] C. A. Broderick, M. Usman, S. J. Sweeney, and E. P. O. O'Reilly, Semicond. Sci. Technol. **27**, 094011 (2012).

[6] D. L. Young, J. F. Geisz, and T. J. Coutts, Appl. Phys. Lett. **82**, 1236 (2003).

[7] B. Fluegel, S. Francoeur, A. Mascarenhas, S. Tixier, E. C. Young, and T. Tiedje, Phys. Rev. Lett. **97**, 067205 (2006).

[8] S. J. Sweeney, Z. Batool, K. Hild, S. R. Jin, and T. J. C. Hosea, *13th International Conference on Transparent Optical Networks (ICTON)* (IEEE, Stockholm, 2011), pp. 1–4.

[9] R. Kudrawiec, J. Kopaczek, P. Sitarek, J. Misiewicz, M. Henini, and S. V. Novikov, J. Appl. Phys. **111**, 066103 (2012).

[10] W. Shan, W. Walukiewicz, J. W. Ager III, E. E. Haller, J. F. Geisz, D. J. Friedman, J. M. Olson, and S. R. Kurtz, Phys. Rev. Lett. **82**, 1221 (1999).

[11] K. Alberi, J. Wu, W. Walukiewicz, K. M. Yu, O. D. Dubon, S. P. Watkins, C. X. Wang, X. Liu, Y.-J. Cho, and J. Furdyna, Phys. Rev. B **75**, 045203 (2007).

[12] M. Usman, C. A. Broderick, A. Lindsay, and E. P. O. O'Reilly, Phys. Rev. B **84**, 245202 (2011).

[13] H.-X. Deng, J. Li, S.-S. Li, H. Peng, J.-B. Xia, L.-W. Wang, and S.-H. Wei, Phys. Rev. B **82**, 193204 (2010).

[14] H. Yaguchi, S. Miyoshi, G. Biwa, M. Kibune, K. Onabe, Y. Shiraki, and R. Ito, J. Cryst. Growth **170**, 353 (1997).

[15] V. Virkkala, V. Havu, F. Tuomisto, and M. J. Puska, Phys. Rev. B **88**, 035204 (2013).

[16] P. J. Klar, H. Grüning, W. Heimbrodt, J. Koch, F. Höhnsdorf, W. Stolz, P. M. A. Vicente, and J. Camassel, Appl. Phys. Lett. **76**, 3439 (2000).

[17] A. Janotti, S.-H. Wei, and S. B. Zhang, Phys. Rev. B **65**, 115203 (2002).

[18] Y. Zhang, A. Mascarenhas, and L.-W. Wang, Phys. Rev. B **71**, 155201 (2005).

[19] G. Kresse and J. Furthmüller, Comput. Mater. Sci. **6**, 15 (1996).

[20] G. Kresse and D. Joubert, Phys. Rev. B **59**, 1758 (1999).

[21] Our hybrid functional calculations were performed using the HSE06 hybrid functional. The Hartree-Fock mixing constant was adjusted to 31% to reproduce the experimental bulk band gap at 0 K in GaAs and the corresponding optimized lattice parameter was 5.68 Å. For the HSE range separation parameter μ we use a value of 0.2/Å. The SO coupling was not included in HSE06 calculations. In HSE06 calculations the studied system was the Ga$_{32}$As$_{31}$Bi supercell.

[22] I. Vurgaftman, J. R. Meyer, and L. R. Ram-Mohan, J. Appl. Phys. **89**, 5815 (2001).

[23] Z. Batool, K. Hild, T. J. C. Hosea, X. Lu, T. Tiedje, and S. J. Sweeney, J. Appl. Phys. **111**, 113108 (2012).

[24] V. Popescu and A. Zunger, Phys. Rev. Lett. **104**, 236403 (2010).